Characterization of blood flow rate in dental pulp by speckle patterns of backscattered light from an *in vivo* tooth

Sergey K. Dick
Galina G. Chistyakova
Alex S. Terekh
Alex V. Smirnov
Mehrnush M. Salimi Zadeh
Vladimir V. Barun

Characterization of blood flow rate in dental pulp by speckle patterns of backscattered light from an *in vivo* tooth

Sergey K. Dick,[a] **Galina G. Chistyakova,**[b] **Alex S. Terekh,**[a] **Alex V. Smirnov,**[a] **Mehrnush M. Salimi Zadeh,**[a] **and Vladimir V. Barun**[a,c,*]
[a]Belarus State University of Informatics and Radioelectronics, Brovka Street 6, Minsk 220013, Belarus
[b]Belarus State Medical University, Dzerzhinskiy Avenue 83, Minsk 220116, Belarus
[c]Belarus National Academy of Sciences, B.I. Stepanov Institute of Physics, Nezavisimosti Pr. 68, Minsk 220072, Belarus

Abstract. Experimental data on the hemodynamics of dental pulp at different stages of caries treatment are given. Observations of speckle patterns in backscattered laser light are used as a measurement method to qualitatively characterize changes in blood flow rate through the dental pulp. The measurements were made by the author-designed experimental setup. Theoretical estimations showed that stationary reflected light from an *in vivo* tooth contains a negligibly small information body on changes in the pulpal blood flow due to the shadowing of the pulp by optically thick enamel and dentin. Therefore, the temporal variations in the speckle patterns are the only possible way that can provide monitoring of blood conditions in the pulp by using backscattered light. Various statistical characteristics of the random reflected light fields are studied as indicators of blood flow rate changes. There were selected five statistical parameters of backscattered speckle images that give self-consistent data on these changes. The parameters include four combinations of integrals of the Fourier transforms of the observed temporal variations as well as the speckle image contrast. The selected parameters are shown to qualitatively agree with general considerations on the effects of reduced or increased blood flow rates on the selected integral quantities. © *2014 Society of Photo-Optical Instrumentation Engineers (SPIE)* [DOI: 10.1117/1.JBO.19.10.106012]

Keywords: tooth tissue; dental pulp; blood flow rate; speckle; caries treatment; backscattered light.

Paper 140363RR received Jun. 9, 2014; revised manuscript received Sep. 24, 2014; accepted for publication Sep. 24, 2014; published online Oct. 23, 2014.

1 Introduction

Pulp status is of great importance for diagnosing the health conditions of a tooth, because the pulp performs various essential functions, such as formative, nutritive, sensory, protective ones, and so on. There are various known methods for testing pulp vitality. Among them are thermal and electric measurements, pulse oximetry (PO), laser Doppler flowmetry (LDF), and others. One can mention recently published reviews,[1–7] which simplify these methods, compare them, and discuss their advantages and drawbacks. Thermal and electric tests assess the response of a tooth to a corresponding stimulus. These methods are the most common ones employed by dentists in clinics, but are rather qualitative, subjective, and specific to a patient. The PO and LDF optical tests are designed to measure blood vascular supply or the microcirculation of a tooth. They are objective and noninvasive methods to be based, respectively, on different light absorption of oxy and deoxyhemoglobin in the red or near infrared (IR) and on the Doppler effect. The latter reveals itself as a frequency shift of light scattered by moving blood erythrocytes.

There also exist theoretical and experimental techniques as well as corresponding measuring methods and equipment to study blood flow or hemodynamics by optical means[8–10] based on the interference of the coherent light reflected from

a biological medium. Reflected light contains so-called speckles which are a combination of dark and bright spots. The speckles are of a random temporal character due to pseudo-randomly changing blood velocity directions and mutual positions of moving particles. As a result, the interference pattern of light scattered by erythrocytes fluctuates in time, so that the frequency of such fluctuations depends, among a lot of many other reasons, on the particle velocities and characterizes the desired blood flow rate. The said principles are really implemented in various experimental setups and schemes as applied to soft biological tissues.[11–17] The operating range of such methods is on the order of several light penetration depths. For example, in skin, the depth can vary from fractions of a millimeter to one centimeter[10,18] as a function of the visible to near-IR wavelength used to form speckles. With regard to hard tooth tissues, the optical speckle methods are mainly used for investigating stresses and deformations in a tooth under treatment by various means.[19,20] Here, the informative tool is not the spot fluctuations, but the changes in speckle patterns of the reflected light from unloaded and loaded illuminated tissues. The patterns are essentially stationary because they are formed by coherent photons scattered in enamel and dentin. There are no moving biological particles in hard tissue layers. Within a tooth, moving erythrocytes are present only in dental pulp, but the pulp is highly shadowed by the two upper optically thick layers. The depth of the pulp below the tooth surface is much greater

*Address all correspondence to: Vladimir V. Barun, E-mail: barun@dragon.bas-net.by

than the light penetration depth in tooth tissue. We will give some estimations of this physical quantity below. The above shadowing is the reason why pulpal blood makes a negligible contribution to backscattered stationary light fluxes. This physically transparent fact complicates the extraction of information of blood flow rate in the pulp from speckle patterns. In our opinion, it is the main reason why optical speckle methods are not as widely applied in studying blood flows in tooth pulp as they are in soft biotissues.

Meanwhile, light scattering by moving erythrocytes of tooth pulp should contribute to the frequency spectra of speckle images. The rejection of their stationary background could provide insight into blood flow rates in the pulp. Note that the implementation of the PO and LDF tests also requires some temporal and spectral filtration means to isolate signals at the pulse frequency and at the shifted wavelength. It is the main objective of this paper to illustrate why the stationary light backscattered by tooth tissue contains practically no information on the blood flow in the pulp and, therefore, should be filtered out and how the usage of the alternating current (AC) component of speckle patterns from an *in vivo* tooth promotes the extraction of the data on erythrocyte movement in dental pulp.

2 Materials and Methods

2.1 Simulation Method of Stationary Light Fields Inside and Outside Multilayered Tooth Tissue

Tooth tissue is assumed to be a three-layered medium composed of enamel (top layer), dentin (intermediate layer), and dental pulp (bottom layer). All these layers are highly turbid, so one can represent them as uniform infinite slabs in the direction perpendicular to the light incidence. We will use this assumption in further simulations. Optical and geometrical characteristics of the multilayered medium to describe light fields inside the tissue and backscattered by it must be specified. Unfortunately, there are no so much published data on the scattering and absorption coefficients, μ_s and μ_a, and on the phase function (or its integral parameters) of tooth tissue as there are data concerning soft biotissues. The phase function of each layer is usually represented[21] as the sum of the totally diffuse component (with relative weight f_d) and the Henyey–Greenstein function with relative weight $(1 - f_d)$ and asymmetry parameter g (or the mean cosine of the scattering angle). Several works[21–28] have been devoted to experimental or model estimations of the said optical characteristics at several wavelengths λ.

We used the compilation of data[21,24,26,28] on μ_s, μ_a, f_d, and g for enamel and dentin to simulate spectral light fields inside and outside tooth tissues. For intermediate wavelengths where published results were lacking, the literature data were extrapolated and interpolated as needed. Note that the employed optical model is rough. In particular, it does not take into account the anisotropy of tissue scattering properties caused by the orientations of enamel prisms and dentinal tubules.[29–32] We ignored this effect for our estimations as many investigators do while studying light propagation through tooth tissue.

The dental pulp is the connective tissue. Its main optically essential chromophores are blood, interstitial fluid, collagen bloodless tissue, and some other minor components. The optical properties of the pulp were assumed below to be the same as those of soft biotissues. According to their various models,[33–35] scattering and especially the absorption properties of the soft tissue depend on the blood volume fraction C_V (blood volume per tissue volume). To estimate the value of C_V, let the pulp volume be[36] $V_p = 0.02$ cm^3, pulp density (pulp consists of 75% to 80% water[37]) $\rho_p = 1$ g/cm^3, and specific blood flow through pulp[38] $F_0 = 40$ to 50 mL/min per 100 g of pulp. Then the blood volume $V_b = v_b \cdot \Delta t \cdot S \cdot C_V$ passes through the pulp section area $S \approx (V_p)^{2/3}$ per time Δt, where v_b is the blood velocity in pulp. On the other hand, $V_b = F_0 \cdot \rho_p \cdot V_p \cdot \Delta t$. From these two equations, one can estimate $C_V = 0.025/v_b$ for the specific F_0 value, where v_b is in mm/s. The velocity v_b depends on the blood vessel type and diameter. It approximately equals[39] 0.08 to 0.36, 0.3 to 2.5, and 0.5 to 1 mm/s for capillaries, arterioles, and venules, respectively. Therefore, concentration C_V varies from 0.01 to 0.3. This range agrees rather well with measurements[40] and will be used in the model calculations below.

We simulated the diffuse reflectance (usually measured by an integrating sphere) and depth distributions of the fluence rate over three-layered tooth tissue. The calculation procedure to do so as it applied to skin tissue, was published[18,41,42] earlier. This method is based on the known analytical solutions to the radiative transfer equation,[43] accounting for multiple re-reflections between tissue layers and the surface. The goals of the simulations are to evaluate whether blood conditions will be seen in the reflected light and to estimate the light penetration depth in tooth tissue.

2.2 Experimental Setup

The schematic and general views of the device for monitoring blood microcirculation are shown in Fig. 1. The setup was tested
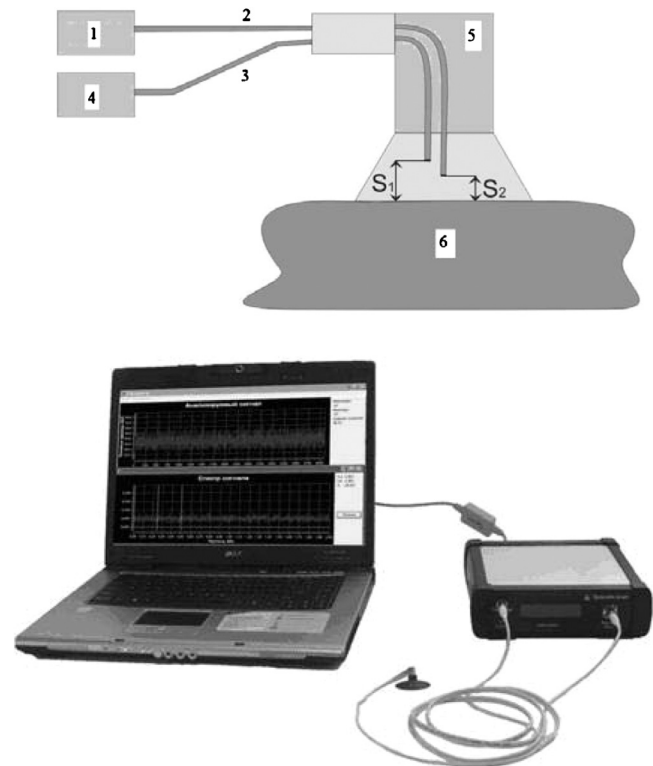
Fig. 1 Schematic (upper part) and general (lower) views of the setup: 1 – laser, 2 – transmitting fiber, 3 – receiving fiber, 4 – recording module, 5 – sensor assembly, 6 – biological object. Distances S_1 and S_2 are selected to form the required sizes of the illuminating and received light beams and to provide the maximal possible contrast of speckle images.

and certified by the Belarus State Institute of Metrology. The setup and study protocols were approved for use on human subjects (Certificate No. IM-7.2263).

The setup[44] includes a laser illuminating module, a recording module, and a processing unit. The illuminating module contains a single-mode semiconductor laser diode HL6501MG conjugated with a single-mode transmitting fiber SM600, a connector FC, a module for monitoring laser power, and a low-voltage power supply. The wavelength of the diode is $\lambda = 660$ nm and the light power is $P_{out} \leq 7.5$ mW at the output of the fiber.

The recording module includes a sensor assembly, a receiving fiber, a photo-electronic multiplier (PEM) (FEU-114), an amplifier, a band-pass filter, an analog-to-digital converter (ADC), and a high-voltage power supply. The sensor assembly contains a special mouth piece providing a nondisturbing contact between the assembly and the tissue surface. The mouth piece [shown in the lower part of Fig. 1(b) as applied to skin tissue] also serves as a screen for light scattered by adjacent areas of the object studied. The PEM is supplied by high voltage to provide the required spectral sensitivity (about 10^{-10} lm/Hz) of the sensor. The PEM outputs an electric signal to the amplifier with a controllable gain that properly amplifies it for the ADC. The filter rejects the DC component of the PEM signals and restricts their frequency band within a controllable range. The ADC digitizes the analog signal from the filter and delivers the output to the processing unit.

The latter includes a PC and operating software. It controls the amplifier's gain and the filter band and performs the pre- and final processing operations. These operations include gathering the experimental data, their Fourier transform, and statistical processing of the results obtained. The filter band is usually set to transmit frequencies in the range of 10 to 2000 Hz.

2.3 Patients

Dental care was provided for patients with a diagnosis of deep or middle occlusal caries. The patients were referred by themselves to a dental establishment. They volunteered for the study and the proper consent was obtained. The x-ray studies of the teeth have shown that the distances between the bottoms of carious cavities and the pulp cameras were 1.5 to 2 mm. All the *in vivo* teeth used for the measurements were separated into the following two groups (the number of the teeth in each group is indicated in brackets):

Group 1. Sequential measurements before anesthesia—immediately after anesthesia—in 2 h after anesthesia for deep caries (12); and

Group 2. During middle caries treatment: sequential measurements before preparation, after preparation, after etching, after restoration, after irradiation, and after polishing (10). No anesthesia was used for this group by the approbation of the patients.

2.4 Parameters of Speckle Patterns

The temporal dependences of a light signal backscattered by a multilayered *in vivo* tooth tissue were measured at different stages of caries treatment. Then the speckle patterns were preprocessed (filtered, time- or space-averaged, etc.). Two kinds of parameters were investigated. They are spectral (items a to d below) and spatial characteristics (e). Note that assuming the ergodicity hypothesis in respect to the temporal and spatial

distributions of the speckles, one can replace the space averaging with the time averaging. Then after making the Fourier-transform $W(f)$ (f is the frequency) of the preprocessed temporal signal, the following integral quantities of the transform were calculated as

(a) spectral power

$$S = \int_{f_{min}}^{f_{max}} W(f) df, \quad (1)$$

(b) band coefficient

$$K_b = \int_{f_3}^{f_4} W(f) df / \int_{f_1}^{f_2} W(f) df, \quad (2)$$

(c) coefficient μ

$$\mu = \int_{f_{low}-\Delta f}^{f_{low}+\Delta f} W(f) df / \int_{f_{high}-\Delta f}^{f_{high}+\Delta f} W(f) df, \quad (3)$$

(d) and mean frequency

$$\langle f \rangle = \int_{f_{min}}^{f_{max}} W(f) f df / S. \quad (4)$$

In Eqs. (1) to (4), f_{min} and f_{max} are the minimal and maximal frequencies used in the calculations, f_1, f_2, f_{low}, and f_3, f_4, f_{high} are the frequencies taken, respectively, in the low- and high-frequency regions, and $\Delta f = 10$ Hz is the fixed increment.

We also calculated (after the time averaging of the signals) (e) contrast C of a speckle pattern, which is defined as the ratio of the standard deviation σ of the illuminance I in the observation plane to the background or mean illuminance $\langle I \rangle$ (here brackets $\langle \ldots \rangle$ denote space averaging)

$$C = \sigma / \langle I \rangle = \sqrt{\langle I^2 \rangle - \langle I \rangle^2} / \langle I \rangle. \quad (5)$$

Additionally, other characteristics, such as autocorrelation function, asymmetry coefficient of the spectrum with respect to the mean frequency, $A = \int_{f_{low}}^{\langle f \rangle} W(f) df / \int_{f_{low}}^{f_{high}} W(f) df$, and the ratio of the asymmetry coefficient to the mean frequency, were tested. However, these parameters showed large dispersions and did not enable one to clarify the general relations between them and blood flow rate. For this reason, only the quantities of items (a) to (e) will be used.

3 Results

3.1 Simulated Stationary Reflectance/Fluence Rate

Figure 2 shows the simulations of spectral diffuse reflectance [Fig. 2(a)] and fluence rate distributions over depth z [Fig. 2(b)]. Figure 2(a) gives the calculations for varying enamel thickness d_e and a specific dentin thickness $d_d = 4$ mm. The similar results obtained for other d_d values show that dentin with $d_d > 2$ mm can be practically regarded as an infinitely thick layer with respect to light reflection. In other words, the diffuse reflectance in the visible to the near IR is essentially independent of d_d in this case. This is apparently due to the rather large optical thickness of dentin. For the same reason, the diffuse reflectance
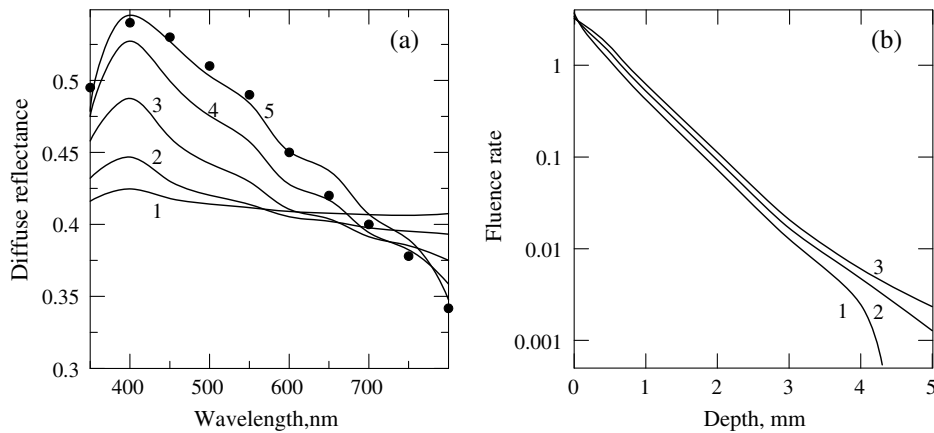
Fig. 2 (a) Spectral dependence of tooth diffuse reflectance, calculations (curves 1 to 5) and experiment[23] (symbols), $d_e = 0.2$ (1), 0.4 (2), 0.8 (3), 1.6 (4), and 3.2 mm (5), $d_d = 4$ mm; and (b) depth dependence of normalized fluence rate inside tooth tissue at $\lambda = 450$ (1), 632 (2), and 800 nm (3), $d_e = 0.2$ mm, $d_d = 4$ mm, $C_V = 0.15$, blood oxygen saturation 0.75.

is independent of blood volume content C_V. This tells us that it is impossible to monitor blood conditions using stationary backscattered light or habitual spectral photometric measurements "by reflection." The situation is understood to be opposite when one observes transmitted light. In such a case, this light can be promoted to monitor various blood parameters.[39,45] Figure 2(a) also gives the experimental data[23] on diffuse reflectance (symbols). One can see that the experimental results show a behavior similar to our theoretical simulations. This is surprising at the first glance, if one recalls that the base for the calculations is a rather rough optical model.

Depth dependences of the fluence rate are shown in Fig. 2(b). Here, the ordinate data are dimensionless so as to be normalized by the incident power density. One can see that fluence rate near the tooth surface up to some fractions of mm is greater than unity. This is due to the large amount of backscattered light at the topical tooth region. Note two points with respect to Fig. 2(b). First, the fluence rate in the pulp at the blue—violet wavelengths attenuates quickly with depth because of high blood absorption there. In the red to near IR, blood absorption is lower, and the shown dependences, for all practical purposes, do not change their slope. Second, one can roughly estimate the light penetration depth z_0 in tooth tissue, which is on the order of 2 mm in the visible to near IR. Here, z_0 values are assumed to be the depths where the fluence rate decreases by 10 times as compared with that incident to the tooth surface.

3.2 Experimental Characterization of Dental Pulp Hemodynamics

For each tooth the parameters of Eqs. (1) to (5) were obtained. Twelve ranges were checked for the spectral power and the band coefficient, 15 for the μ coefficient, and 10 for the mean frequency to select the integration limits of Eqs. (1) to (4). The most informative limits will be given below. The measurements for each tooth were repeated 10 times. Data dispersion was peculiar to each observation so that particular measurements were excluded from the experimental dataset if they were characterized by large deviations of all parameters from the mean results in all considered frequency ranges. On average, 2 to 4 observations were excluded from 10 repetitions. Data for one

tooth were excluded for *Groups 1* and *2* because the corresponding results did not agree with the others.

Then for each *Group* of tested teeth and for each stage of caries treatment, the mean values of the said parameters and their standard deviations were calculated. They are shown below as, respectively, the ordinates of the bar graphs and the error bars in Figs. 3 to 5. The statistical significance of the differences in the parameters at each stage of caries treatment was evaluated according to the well-known Student's t-test. The significance level (p-value) for all the parameters and for all stages was less than 0.01. For specific parameters and specific stages, the p-values were less than 0.001.

Figures 3 and 4(a) show the diagrams of changes in the above parameters observed in experiments with the teeth of *Group 1*, namely before anesthesia (1), immediately after the anesthesia (2), and 2 h after anesthesia (3). Anesthesia will obviously give rise to a reduced blood flow rate. Two h after anesthesia, the spectral power slowly recovers. A similar conclusion can be made from the comparison of the data for $f_{\text{low}} = 100$ and 50 Hz in Fig. 3(c).

Changes in speckle contrast [Fig. 4(a)] also testify to the above qualitative estimations of the speckle image contrast at varying blood flows. Immediately after the anesthesia, the contrast increases due to the obvious reduction in blood flow. However, the contrast becomes even lower than its initial value 2 h after the anesthesia. The latter qualitatively tells us that the blood flow rate is higher in this case compared with its values before treatment. This fact disagrees somewhat with the data of Fig. 3 and requires further investigations.

Figures 4(b) and 5 illustrate the changes in the considered integral parameters of the speckle structure at various stages of caries treatment, namely before (1) and after the preparation (2), after etching (3), after tooth restoration (4), after irradiation (5), and after polishing (6). These stages are correspondingly shown from the left to right. The data on the changes in the speckle contrast, Fig. 4(b), highly correlate (synchronously decrease and increase at the illustrated stages) with those on S and μ values, Figs. 5(a) and 5(c). On the other hand, these results anticorrelate with the data of Figs. 5(b) and 5(d), i.e., when the contrast increases, K_b and $\langle f \rangle$ decrease, and vice versa. A similar correlation and anticorrelation can be mentioned with respect to the corresponding data shown in Fig. 3.
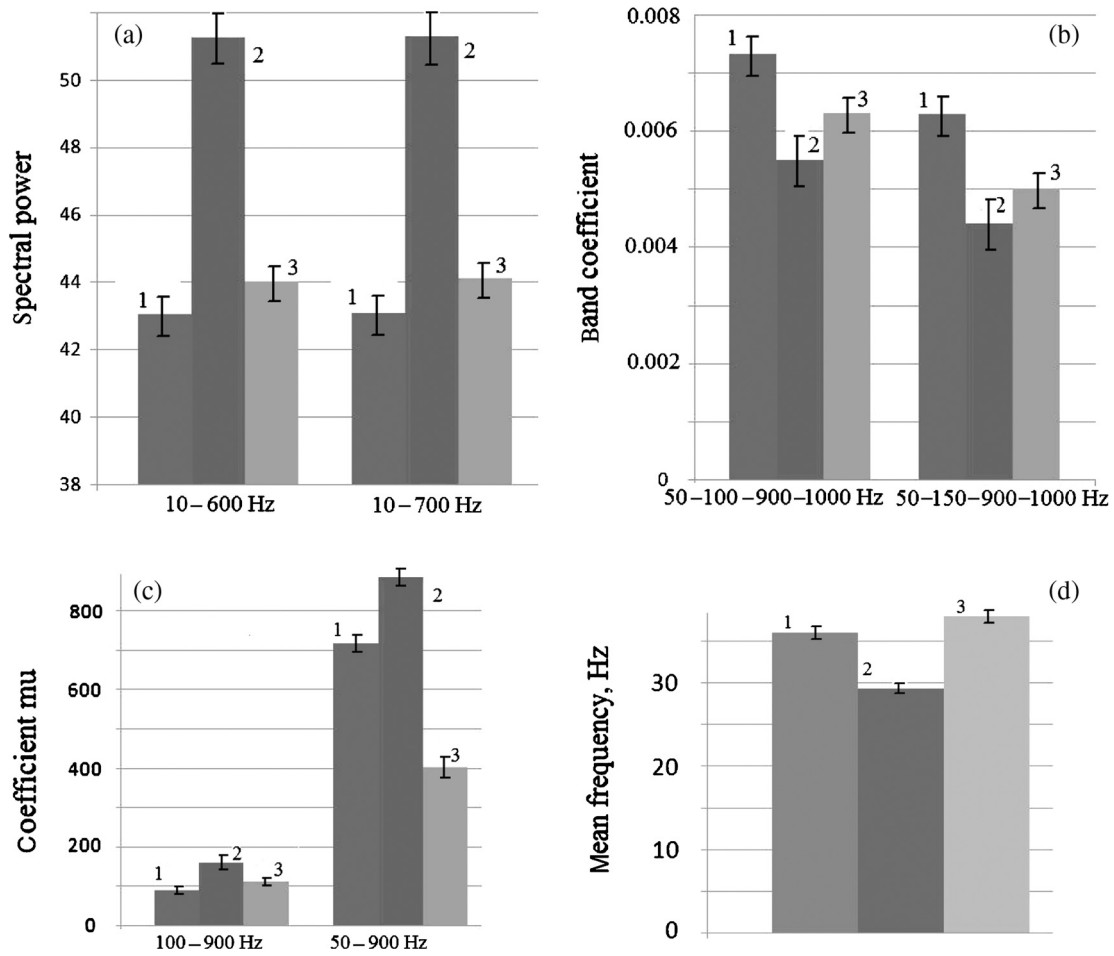
Fig. 3 Changes in spectral power, relative units (a), band coefficient (b), coefficient μ (c), and mean frequency, Hz (d) for an "average" tooth from *Group 1*: (a) $f_{min} = 10$ and $f_{max} = 600$ (or 700) Hz; (b) $f_1 = 50$, $f_2 = 100$ (or 150), $f_3 = 900$, and $f_4 = 1000$ Hz; (c) $f_{low} = 100$ (or 50) and $f_{high} = 900$ Hz; and (d) $f_{min} = 10$ and $f_{max} = 800$ Hz before (1), immediately after anesthesia (2), and in 2 h after anesthesia (3).
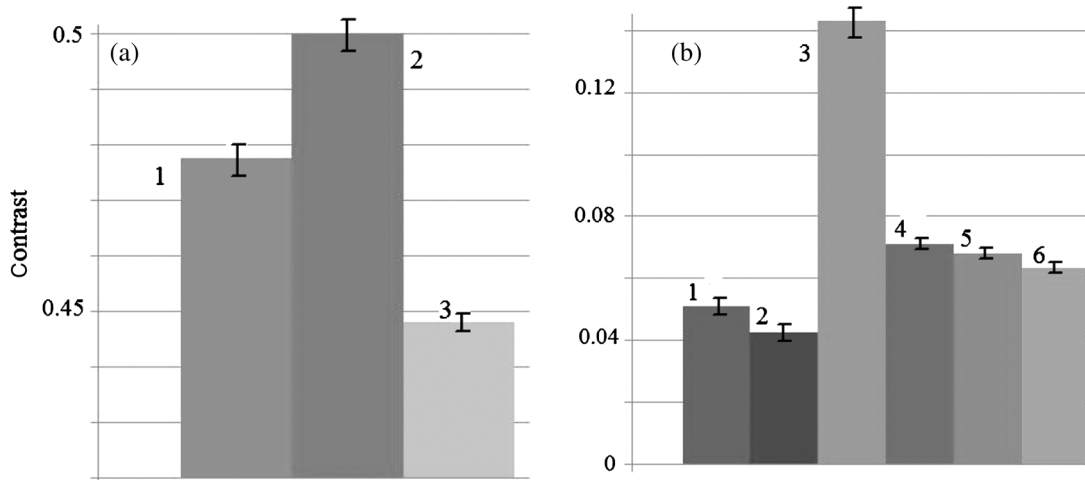
Fig. 4 Changes in speckle contrast (a) before (1), immediately after anesthesia (2), and in 2 h after anesthesia (3) for teeth from *Group 1*; and (b) before (1) and after the preparation (2), after etching (3), after tooth restoration (4), after irradiation (5), and after polishing (6) for teeth from *Group 2*.
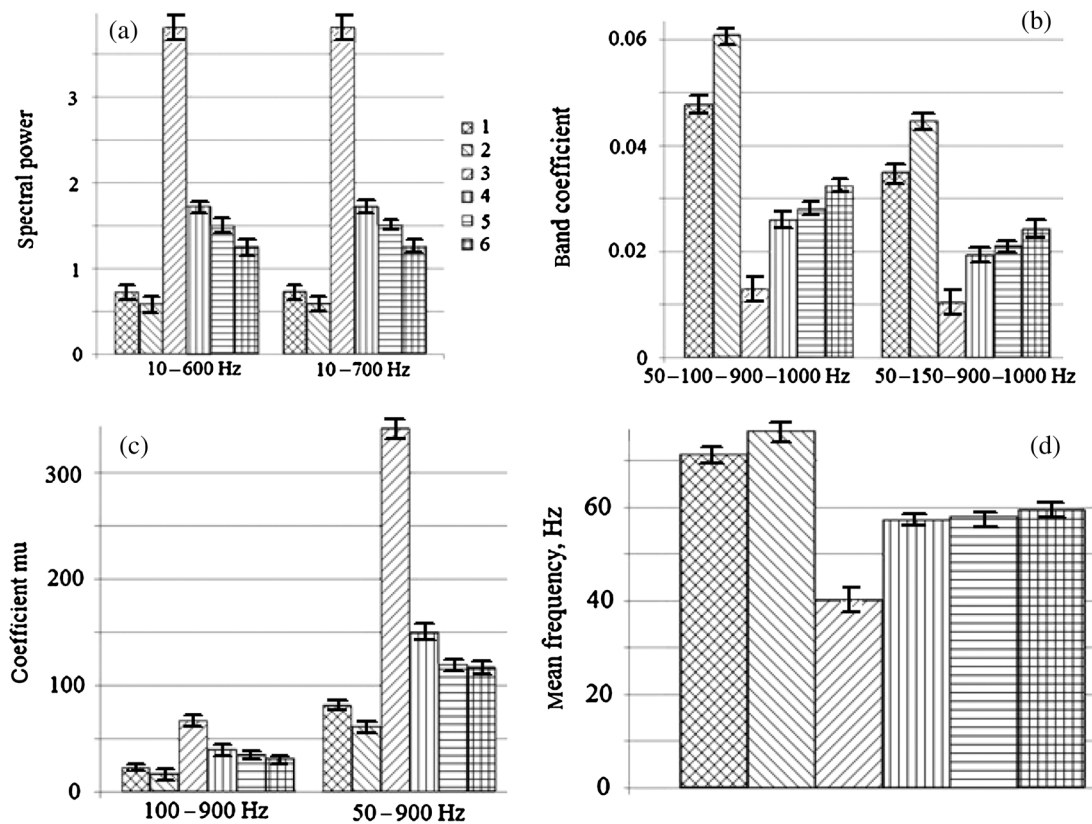
Fig. 5 Changes in spectral power, relative units (a), band coefficient (b), coefficient μ (c), and mean frequency, Hz (d) before (1) and after the preparation (2), after etching (3), after tooth restoration (4), after irradiation (5), and after polishing (6) of a tooth from *Group 2*. (a) $f_{min} = 10$ and $f_{max} = 600$ (or 700) Hz, (b) $f_1 = 50$, $f_2 = 100$ (or 150), $f_3 = 900$, and $f_4 = 1000$ Hz, (c) $f_{low} = 100$ (or 50) and $f_{high} = 900$ Hz, (d) $f_{min} = 10$ and $f_{max} = 800$ Hz. The legend is shown in Fig. 5(a).

4 Discussion

As shown in Sec. 2.1, backscattered light signals without any kind of filtration are practically insensitive to pulp blood conditions. It is understood from the data of Fig. 2(b) why blood optical characteristics do not show themselves in stationary diffuse reflectance. The point is that a highly attenuated light power (by 3 to 4 orders of magnitude depending on the enamel and dentin thicknesses) reaches the pulp to make a negligible contribution to the backscattered fluxes. On the other hand, the data of Figs. 3 to 5 testify that some changes in the parameters of backscattered speckle images (Fourier-frequency filtered) actually occur.

Let us qualitatively evaluate what will happen with the characteristics of Eqs. (1) to (5) as blood velocity changes. When erythrocytes move slower, Fourier transform $W(f)$ is understood to shift to the lower frequency region. This shift is obvious if one recalls that for completely fixed scatterers, the transform will be the Dirac delta-function at $f = 0$, because no temporal fluctuations in the speckle patterns will be observed from immobile particles. The band coefficient of Eq. (2) should, hence, decrease due to the larger denominator and smaller numerator in this case. The μ coefficient of Eq. (3), vice versa, should increase for the same reasons. The spectral power and mean frequency depend on the f_{max} value used in processing the experimental data. Here, one can isolate two cases. (a) If range $f > f_{max}$ outside the integration limits of Eq. (1) contains a high enough spectral power, then for slower moving scatterers,

S should increase due to the redistribution of the power from the high-frequency region to the low-frequency one. (b) Otherwise, the S value will change slightly. The mean frequency of Eq. (4) will show the opposite behavior in case (a), because the denominator of Eq. (4) increases more than the numerator. However, the decrease in $\langle f \rangle$ will be less apparent than the increase in S values due to both the numerator and the denominator increasing for fixed scatterers. In other words, if the S values become doubled, the reduction in the $\langle f \rangle$ values will be perhaps 1.5 times. In case (b), the mean frequency will not substantially change since both the denominator and the numerator are about the same at a reduced blood flow rate. As to the speckle contrast, it is understood from general physical viewpoints that a higher erythrocyte velocity provides a lower image contrast due to the blurring of a single speckle over a larger spatial area.

The experimental data of Figs. 3 to 5 illustrate these qualitative statements and show that the general considerations agree well with the measurements. For example, S and μ values increase at a reduced blood flow, but K_b and $\langle f \rangle$ decrease. Essentially, the same values of S at $f_{max} = 600$ and 700 Hz [left and right histograms in Fig. 3(a)] show that the range of 600 to 700 Hz contains a negligible spectral power that is concentrated at lower frequencies. Besides, the data of Fig. 3(b) enable the distribution of the spectral power over the low-frequency range to be further simplified. One can easily find by comparing the data at $f_2 = 100$ and 150 Hz [left and right columns in Fig. 3(b)] that histograms 1 to 3 correspond

to the ratios of $\int_{100\,\text{Hz}}^{150\,\text{Hz}} W(f)\mathrm{d}f / \int_{50\,\text{Hz}}^{100\,\text{Hz}} W(f)\mathrm{d}f = 0.16$, 0.28, and 0.24, respectively. In other words, these data show that the spectral power immediately after anesthesia is redistributed from a high-frequency range to the range of 100 to 150 Hz.

Other examples can be given to illustrate the opportunities of the approach used in this work to not only differentiate necrotic pulp from vital pulp, but also to study the blood supply in pulp and to measure the pulp vitality under various stages of caries treatment. The speckle method described here can provide quantitative tools for evaluating pulpal vascular responses to external physical and chemical stimuli.

In conclusion, we would like to underline that blood flow vividly responds to mechanical and chemical actions during the treatment of deep dentin caries. According to the gathered data, the most noticeable effect is caused by the etching that strongly depresses the tooth hemodynamics. In practical medicine and in biomedical optical science, it is highly desirable to propose a quantitative explanation of the measured parameters, which enables one to directly relate their values to blood flow quantities. This is our future objective, which will be based on the theoretical model of the speckle formation in backscattered light images of tooth tissue containing moving biological particles.

Acknowledgments

References

1. E. Chen and P. V. Abbot, "Dental pulp testing: a review," *Int. J. Dent.* **2009**, 1–12 (2009).
2. V. Gopikrishna, G. Pradeep, and N. Venkateshbabu, "Assessment of pulp vitality: a review," *Int. J. Paediatr. Dent.* **19**, 3–15 (2009).
3. H. Jafarzadeh, "Laser Doppler flowmetry in endodontics: a review," *Int. Endod. J.* **42**, 476–490 (2009).
4. D. J. Vaghela and A. A. Sinha, "Pulse oximetry and laser Doppler flowmetry for diagnosis of pulpal vitality," *J. Interdiscip. Dent.* **1**, 14–21 (2011).
5. G. N. Baiju et al., "A review of laser Doppler flowmetry and pulse oximetry in dental pulp vitality," *J. Clin. Diag. Res.* **5**, 903–905 (2011).
6. H. Karayilmaz et al., "Comparison of the reliability of laser Doppler flowmetry, pulse oximetry and electric pulp tester in assessing the pulp vitality of human teeth," *J. Oral Rehabil.* **38**, 340–347 (2011).
7. L. Yu. Orekhova and A. A. Barmasheva, "Doppler flowmetry as a tool of predictive, preventive and personalised dentistry," *EPMA J.* **4**, 21–29 (2013).
8. A. P. Shepherd and P. A. Oberg, Eds., *Laser Doppler Blood Flowmetry*, Kluwer Academic Publisher, Boston, MA (1989).
9. N. Fomin, *Speckle Photography for Fluid Mechanics Measurements*, Springer Verlag, Berlin (1998).
10. V. V. Tuchin, Ed., *Handbook of Optical Biomedical Diagnostics*, SPIE Press, Bellingham, WA (2002).
11. C. Riva, B. Ross, and G. B. Benedek, "Laser Doppler measurements of blood flow in capillary tubes and retinal arteries," *Invest. Ophtalmol. Visual Sci.* **11**, 936–944 (1972).
12. M. D. Stern, "In vivo evaluation of microcirculation by coherent light scattering," *Nature* **254**, 56–58 (1975).
13. T. Tanaka and G. B. Benedek, "Measurement of velocity of blood flow (in vivo) using a fiber optical catheter and optical mixing spectroscopy," *Appl. Opt.* **14**, 189–196 (1975).
14. M. D. Stern, "Laser Doppler velocimetry in blood and multiply scattering fluids: theory," *Appl. Opt.* **24**, 1968–1986 (1985).
15. S. S. Ul'yanov, "A new type of manifestation of Doppler effect. An application to blood and lymph flow measurements," *Opt. Eng.* **34**(10), 2850–2855 (1995).
16. J. D. Briers, "Laser Doppler and time-varying speckle: a reconciliation," *J. Opt. Soc. Am. A* **13**, 345–350 (1996).
17. J. D. Briers, "Laser Doppler, speckle and related techniques for blood perfusion mapping and imaging," *Physiol. Measur.* **22**, R35–R66 (2001).
18. V. V. Barun et al., "Absorption spectra and light penetration depth of normal and pathologically altered human skin," *J. Appl. Spectrosc.* **74**, 430–439 (2007).
19. R. Jones and C. Wykes, *Holographic and Speckle Interferometry*, Cambridge University Press, Cambridge (1983).
20. N. A. Fomin, S. P. Rubnikovich, and N. B. Bazylev, "New possibilities of investigating blood flow in soft tissues of the mouth," *J. Eng. Phys. Thermophys.* **81**, 533–543 (2008).
21. D. Fried et al., "The Nature of light scattering in dental enamel and dentin at visible and near-IR wavelengths," *Appl. Opt.* **34**, 1278–1285 (1995).
22. D. Spitzer and J. J. ten Bosch, "The absorption and scattering of light in bovine and human dental enamel," *Calcif. Tissue Res.* **17**, 129–137 (1975).
23. J. R. Zijp and J. J. ten Bosch, "Angular dependence of He–Ne laser light scattering by bovine and human dentine," *Arch. Oral Biol.* **36**, 283–289 (1991).
24. J. R. Zijp and J. J. ten Bosch, "Theoretical model for the scattering of light by dentin and comparison with measurements," *Appl. Opt.* **32**, 411–415 (1993).
25. J. R. Zijp, J. J. ten Bosch, and R. A. Groenhuis, "He–Ne Laser light scattering by human dental enamel," *J. Dental Res.* **74**, 1891–1898 (1995).
26. J. Vaartkamp, J. J. ten Bosch, and E. H. Verdonschot, "Light propagation through teeth containing simulated caries lesions," *Phys. Med. Biol.* **40**, 1375–1387 (1995).
27. J. R. Zijp, "Optical properties of dental hard tissues," Ph.D. Thesis, Groningen, The Netherlands (2001).
28. D. Fried, M. Staninec, and C. L. Darling, "Near-infrared imaging of dental decay at 1310 nm," *J. Laser Dent.* **18**, 8–16 (2010).
29. G. B. Altshuler and V. N. Grisimov, "New optical effects in the human hard tooth tissues," *Proc. SPIE* **1353**, 97–102 (1991).
30. V. M. Zolotarev and V. N. Grisimov, "Architectonics and optical properties of dentin and dental enamel," *Opt. Spectrosc.* **90**, 753–759 (2001).
31. A. Kienle, R. Michels, and R. Hibst, "Magnification: a new look at a long-known optical property of dentin," *J. Dent. Res.* **85**, 955–959 (2006).
32. A. Kienle and R. Hibst, "Light guiding in biological tissue due to scattering," *Phys. Rev. Lett.* **97**, 018104 (2006).
33. V. V. Tuchin, "Light scattering study of tissues," *Phys. – Usp.* **40**, 495–515 (1997).
34. V. V. Barun and A. P. Ivanov, "Thermal effects of a short light pulse on biological tissues. I. An optical—thermophysical model," *Biophysics* **49**, 1004–1012 (2004).
35. S. L. Jacques, "Optical properties of biological tissues: a review," *Phys. Med. Biol.* **58**, R37–R61 (2013).
36. Pulp (tooth), 2014, http://en.wikipedia.org/wiki/Pulp_(tooth) (25 May 2014).
37. Dental pulp, 2001, http://www.uky.edu/~brmacp/oralhist/module4/lecture/oh4lectm.htm (25 May 2014).
38. C. Yu and P. V. Abbott, "An overview of the dental pulp: its functions and responses to injury," *Aust. Dental J.* **52**(1 Suppl.), S4–S16 (2007).
39. S. Kim et al., "Arteriovenous distribution of hemodynamic parameters in the rat dental pulp," *Microvasc. Res.* **27**, 28–38 (1984).
40. N. Vongsavan and B. Mattews, "The vascularity of dental pulp in cats," *J. Dental Res.* **71**, 1913–1915 (1992).
41. V. V. Barun and A. P. Ivanov, "Light and thermal fields in multilayer skin tissue exposed to laser irradiation," *Opt. Spectrosc.* **100**, 139–147 (2006).
42. V. V. Barun and A. P. Ivanov, "Light absorption in blood during low-intensity laser irradiation of skin," *Quantum Electron.* **40**, 371–376 (2010).
43. E. P. Zege, A. P. Ivanov, and I. L. Katsev, *Image Transfer through a Scattering Medium*, Springer-Verlag, Heidelberg (1990).
44. S. K. Dick et al., "Speckle optical devise for evaluation of the surface state of blood flow and biomechanical parameters of muscles," Belarus Patent No. BY 14011 C1 (2010).

45. A. M. Diaz-Arnold, L. R. Wilcox, and M. A. Arnold, "Optical detection of pulpal blood," *J. Endod.* **20**, 164–168 (1994).

Sergey K. Dick is a dean of the computer design department of the Belarus State University of Informatics and Radioelectronics, Minsk, Belarus. He received his PhD degree in physics and mathematics at the Institute of Physics, Belarus National Academy of Sciences. His research interests include biophotonics, application of interferometric methods for studying living tissues, and design of optical devices as applied to biomedical purposes.

Galina G. Chistyakova is an assistant professor at the Belarus State Medical University Minsk, Belarus. She received her PhD degree in medicine. Her research interests include design of new biomedical methods for tooth caries treatment, application of various physical/optical innovations in dentistry, and practical usage of optical devices for dental purposes.

Alex S. Terekh is a PhD student in the computer design department of the Belarus State University of Informatics and Radioelectronics, Minsk, Belarus. His research interests include design, production, and practical usage of speckle-based devices for biomedical purposes.

Alex V. Smirnov is a PhD student in the computer design department of the Belarus State University of Informatics and Radioelectronics, Minsk, Belarus. His research interests include design, production, and practical usage of speckle-based devices for biomedical purposes.

Mehrnush M. Salimi Zadeh is a PhD student in the computer design department of the Belarus State University of Informatics and Radioelectronics, Minsk, Belarus. Her research interests include light propagation through biotissues, tissue heating by light irradiation, and experimentation with model and natural biomedical media.

Vladimir V. Barun is a senior researcher at the B.I. Stepanov Institute of Physics, Belarus National Academy of Sciences and Belarus State University of Informatics and Radioelectronics, Minsk, Belarus. His research areas include light propagation through biotissues, development of analytical methods for solving the radiative transfer equation, design of invasive and noninvasive techniques for solving various inverse problems of biomedical optics, and construction of full optical and thermal models of different biotissues.